

## The small GTP-binding protein rab6p is distributed from medial Golgi to the *trans*-Golgi network as determined by a confocal microscopic approach

CLAUDE ANTONY<sup>1,\*</sup>, CHRISTIAN CIBERT<sup>1,2</sup>, GÉRARD GÉRAUD<sup>2</sup>, ANGELICA SANTA MARIA<sup>1</sup>,  
BERNARD MARO<sup>1,2</sup>, VÉRONIQUE MAYAU<sup>3</sup> and BRUNO GOUD<sup>3</sup>

<sup>1</sup>Institut Jacques Monod, Laboratoire de Physiologie du Développement, CNRS-Université Paris VII, 2 Place Jussieu, F-75005 Paris, France

<sup>2</sup>Institut Jacques Monod, Service Commun de Microscopie Confocale, CNRS-Université Paris VII, 2 Place Jussieu, F-75005 Paris, France

<sup>3</sup>Institut Pasteur, Unité de Génétique Somatique (URA CNRS 361), 25 rue du Dr. Roux, F-75015 Paris, France

\*Author for correspondence

### Summary

A key role in the regulation of membrane traffic is played by the rab proteins, members of a family of ras-related small GTP-binding proteins. This family comprises at least 25 identified members, the intracellular localization of only a few of which has been investigated. rab6p has been shown to be distributed along the exocytic pathway in association with the medial and *trans* regions of the Golgi apparatus. A confocal laser scanning microscopic (CLSM) approach coupled with image analysis was used to compare the localization of rab6p with selected reference Golgi markers by double immunofluorescence on culture cell lines. CLSM analysis shows that, under a set of well-defined conditions, one can investigate the possible colocalization of known markers of Golgi compartments and orientate a couple of labeled Golgi antigens with regard to the polarity of the Golgi apparatus. Thus, having validated the CLSM analysis, the localization of rab6p was studied and com-

pared with some of these markers and the VSV-G protein in VSV (vesicular stomatitis virus)-infected cells blocked at 20°C. rab6p is shown to be associated in all the cell lines used with the last cisternae of the Golgi apparatus and particularly with the *trans*-Golgi network (TGN), the site of protein sorting at the exit of the Golgi apparatus. These results were supported by an electron microscopic study using double-immunolabeled cryosections: rab6p was found in some flat cisternae of the Golgi stack and colocalized with the VSV-G protein in the TGN. Our results show that the small GTP-binding protein rab6p is distributed from medial Golgi to TGN along the exocytic pathway.

Key words: membrane traffic, Golgi apparatus, GTP-binding protein, laser scanning confocal microscopy, immuno-electron microscopy.

### Introduction

Membrane and luminal proteins moving along the biosynthetic/secretory pathway from their site of synthesis in the endoplasmic reticulum (ER) to their final destination (plasma membrane or intracellular organelles) cross sequentially a series of membranous compartments, including the intermediate or salvage compartment, the different Golgi compartments and the *trans*-Golgi network (TGN). Inter-organelles and intra-Golgi transports are thought to be mediated by carrier or transport vesicles that bud from one compartment (becoming the donor compartment) and are targeted to and fuse with the next compartment (becoming the acceptor compartment) (Palade, 1975; Rothman and Orci, 1992).

The ordered flow of transport vesicles is dependent on a set of regulatory signals that are responsible for their proper

targeting and fusion to acceptor compartments. A number of studies have recently indicated that small GTP-binding proteins act as major regulators of the targeting/fusion events occurring at each transport step (for review see Goud and McCaffrey, 1991; Pfeffer, 1992). Such a role has been proposed, based on studies of Sec4p and Ypt1p, two ras-like GTP-binding proteins involved in the biosynthetic/secretory pathway of the yeast *Saccharomyces cerevisiae* (Gallwitz et al., 1983; Salminen and Novick, 1987). Indeed, genetic and biochemical evidence indicates that Ypt1p and Sec4p control the targeting and/or fusion of ER-derived transport vesicles (Bacon et al., 1989; Baker et al., 1990; Segev, 1991; Segev et al., 1988) and post-Golgi vesicles with the Golgi apparatus or with the plasma membrane, respectively (Goud et al., 1988; Salminen and Novick, 1987; Walworth et al., 1989). In mammalian cells, products of the so-called *rab* gene family share with

Sec4p/Ypt1p structural similarities in several domains, one of which includes a putative effector region (Chavrier et al., 1990b; Touchot et al., 1987; Zahraoui et al., 1989). Although very little is yet known about the function(s) of rab proteins, it has been suggested that they fulfil functions similar to those of Sec4p/Ypt1p and are thus involved in targeting/fusion events. Data now available for three of the rab proteins support this hypothesis: (i) rab5p is involved in endosome-endosome fusion *in vitro* (Gorvel et al., 1991); (ii) rab1bp, one of the mammalian homologues of Ypt1p (Haubruck et al., 1989), is implicated in targeting/fusion of ER-derived vesicles with the *cis*-Golgi (Plutner et al., 1991); (iii) rab3ap might control the exocytic process of synaptic vesicles in synaptosomes (Fischer von Mollard et al., 1991).

Most of the proteins of the Sec4/Ypt1 family that have been localized so far are found on either transport vesicles and acceptor compartments (for example, Sec4p; Goud et al., 1988), or successive donor and acceptor compartments (for example, rab5p; Chavrier et al., 1990a). These data support the hypothesis that the rab family proteins play a role in specific targeting/fusion events between two adjacent compartments (Bourne, 1988). However, they are not sufficiently conclusive to determine whether the localization of these proteins is really restricted to a single pair of donor/acceptor compartments. In addition, it has been recently shown that rab1bp localization probably extends over ER to Golgi subcompartments (Plutner et al., 1991). We address this issue in the case of rab6p, a ubiquitous protein previously found to be associated with medial and *trans* cisternae of the Golgi apparatus in normal rat kidney cells (NRK) (Goud et al., 1990). The available data on rab6p make it likely that this GTP-binding protein is involved in the regulation of late intra-Golgi transport events.

In this work, our goal was to determine whether rab6p is also present in the TGN, an organelle in which no known small GTP-binding proteins have been identified. For this purpose, the distribution of rab6p was investigated by confocal laser scanning microscopy (CLSM) and compared with the distribution of known intrinsic markers of the Golgi apparatus. We report that CLSM combined with image analysis allows us to distinguish between Golgi compartments and TGN. Using this approach, we were able to show that rab6p is distributed in a polarized fashion in the Golgi apparatus and is associated with the TGN. This was confirmed at the ultrastructural level by the colocalization of rab6p and the G protein of the vesicular stomatitis virus (VSV-G) after a 20°C block in infected cells.

## Materials and methods

### Immunofluorescence

Cells grown on glass coverslips were fixed with 4% paraformaldehyde in PBS or in 250 mM HEPES buffer, pH 7.2, for 10 min, then permeabilized for 30 min with 0.05% saponin in PBS containing 0.3% BSA and 0.2% fish skin gelatin (FSG). The cells were then incubated for 1 h with the various antibodies in PBS containing 0.05% saponin, 0.3% BSA, 0.2% FSG, washed three times in the same buffer, and incubated for 30 min with the appro-

priate goat anti-immunoglobulin antibodies labeled with either fluorescein or rhodamine (KPL inc., Gaithersburg, USA). Finally, the coverslips were rinsed and mounted in a glycerol/PBS solution (Citifluor Ltd., London, UK).

For the double-staining experiments using the 53FC3 monoclonal antibody associated with the various polyclonal antibodies, fixation was with 1.2% formaldehyde in 250 mM HEPES for 10 min, followed by permeabilization with 0.15% saponin prior to incubations with specific and secondary antibodies.

### Antibodies

The various antibodies used in this study were: affinity purified anti-rab6p antibodies, raised against purified recombinant rab6p (Goud and McCaffrey, 1991); a mouse monoclonal anti-VSV (vesicular stomatitis virus)-G protein, P5D4, directed against the carboxy-terminal end of VSV-G (Kreis, 1986); a mouse monoclonal antibody against mannosidase II, a medial-Golgi marker (Burke et al., 1982); a rabbit anti-rat TGN38 (a TGN integral membrane protein) polyclonal antiserum, (Luzio et al., 1990); a polyclonal rabbit antiserum (15C8), raised against a *cis*-medial Golgi antigen (GIMPC) (Yuan et al., 1987).

### Cell culture

NIH/3T3 cells were cultured in Dulbecco's modified Eagle's medium (Gibco, Life Technology Ltd, Paisley, Scotland) containing 10% fetal calf serum (FCS). BHK (clone 21) cells were cultured in Glasgow's minimum essential medium (BHK medium) containing 10% tryptose phosphate broth (Gibco) and 10% FCS. Madin Darby canine kidney cells (MDCK II) were cultured in MEM medium containing 10% FCS. For immunofluorescence the cells were plated on glass coverslips in plastic Petri dishes 48 h prior to the experiment.

### Viral infections

BHK cell monolayers grown on glass coverslips were infected with the temperature-sensitive mutant tsO45 of VSV (20 plaque-forming units (p.f.u.)/cell) by gentle agitation of the cells at room temperature in the presence of the virus for 45 min, followed by 1 h at 33°C and then shifted to 39.5°C for 3 h. The 20°C block was performed by transfer of the Petri dishes to a water bath maintained at 20°C for 2 h in the presence of 10 µg/ml cycloheximide as previously described (Griffiths et al., 1985).

### Confocal microscopy

#### Image acquisition

Confocal laser scanning microscopy was performed using a BioRad MRC-600, mounted on an Optiphot II Nikon microscope equipped with a ×60 objective (Plan apo; NA 1.4). For fluorescein, an argon ion laser (Ion LASER Technology) adjusted at 488 nm wavelength was used, close to the maximum of absorption of fluorescein, and for rhodamine a helium-neon ion laser (Ion LASER Technology) adjusted at 543 nm was used (close to the maximum of absorption of rhodamine). The emitted light was separated by a dichroic mirror (DR565, BioRad), a band-pass filter (540DF30, BioRad) was placed in front of the photomultiplier to collect the fluorescein emission and a long-pass filter (EF600LP, BioRad) was placed in front of the photomultiplier to collect the rhodamine emission. A Kalman filter (8 to 10 scans) was used during image acquisition to decrease electronic background noise. Double fluorescence images were acquired in two passes, fluorescein first, rhodamine second, to avoid any bleeding from one channel into the other. Double-labeled polystyrene beads (diameter 10 µm; Becton-Dickinson) were used to align the laser beams until both images were perfectly superimposed, with an optimal accuracy of about 0.2 µm.

To distinguish between the relative positions of two Golgi com-

partments, we defined a set of confocal acquisition parameters, which took into account Nyquist's principle (Inoue, 1986) and Webb's remarks (Webb and Dorey, 1990), the minimal size of these compartments being close to the limit of resolution of the optical microscope (i.e. 200 nm). The minimum size of the optical confocal probe that can be reached with our confocal stand using the minimum observation pinhole aperture is about 200 nm in the  $x$  and  $y$  directions and 350 nm in the  $z$  direction. Therefore to obtain a "hyper-resolution" (R) in a small region of the cells, we chose to record  $z$ -series of five images under oversampling conditions in the three directions. To oversample in the ( $x$ ,  $y$ ) plane, we used the 60/1.4 objective and the 8 electronic zoom coefficient, which gives each pixel an "apparent" size of about  $48 \times 48 \text{ nm}^2$  in the digitized image. Thus, the ratio between the area of the ( $x$ ,  $y$ ) section of the optical probe and the area of each pixel of the digitized image is about 14. This means that along the  $x$  direction, the oversampling is about 4 ( $200/48$ ). To oversample in the  $z$  direction, we used a step of  $0.1 \mu\text{m}$  between two images. The depth of the total  $z$ -series (5 images) is equal to  $0.4 \mu\text{m}$ , but corresponds to about  $0.75 \mu\text{m}$  of the sample if the size of the optical probe is taken into account. Thus, the oversampling in this direction is about 2 ( $0.75/0.35$ ).

#### Image analysis

A Personal Iris Work Station (4D-25, Silicon Graphic) running the Visilog (Noesis) image analysis software was used. Image analysis was performed on either the first section of each  $z$ -series or the projection of the 5 sections of a  $z$ -series. To define the boundary of the area of interest (labeled with a given antibody) in the confocal sections, we used a conditional threshold filter (top hat) and determined for each image (hexagonal grid) the size of the filter (7 iterations for most images) and the threshold level (20, 255 for most images). The effect of such a filter is shown in Fig. 1, where it is compared with a simple thresholding filter.

In some cases, to eliminate certain elements that were present in the binary images but were not localized in the Golgi area, the binary images were filtered to retain only those particles that were close enough to be considered to be elements of the Golgi apparatus. In all cases, we tested the quality of the binary image by superimposition of the boundary of this image on the original image (see results: Fig. 3).

The overlap of the binary images obtained from the gray level images in the two channels (i.e. red and green) was determined

and the surface of each area (red, green and overlap) was measured.

The compass card approach was used to define the relative position of two markers with regard to their area of overlap. The oriented dilatation of the area of overlap was performed in the 12 directions (increment =  $30^\circ$ ) of the image plane. The area of overlap between the dilated image and the single-stained area of the original image was then measured. The parameter used in the graphic representation is the ratio between these measured areas of overlap for the red and green labels.

#### Statistical analysis

To perform a statistical analysis of the results obtained using this approach, the orientation of the Golgi apparatus was determined using the *Rose of directions* function of the Visilog software. This function allows the calculation of the length of the outline of a binary image in a given direction of the image plane. Since the images were encoded with a hexagonal grid, measurements were made using an increment of  $30^\circ$ . The axis of the Golgi apparatus was defined as the minimum of the *Rose of directions* and oriented from concavity to convexity. The mean and standard deviation were calculated on a series of images (6-10) obtained using the same settings for image acquisition and filtering.

#### Photographs

Photographs were taken using a Nippon Avionics imager on Fujichrome 100 or Kodak T-MAX 100.

#### Electron microscopy

At the end of the  $20^\circ\text{C}$  block, BHK cells were detached from the Petri dishes with proteinase K ( $50 \mu\text{g}/\text{ml}$ ) at  $4^\circ\text{C}$ . The cells were then pelleted and the pellets were fixed with 4% paraformaldehyde in 250 mM HEPES buffer, pH 7.4, for 10 min before being resuspended in 8% paraformaldehyde for 30 min in the same buffer and pelleted again. Finally, the pellets were infiltrated with 2.1 M sucrose in PBS, pH 7.4, for 20 min, mounted on holders and then frozen in liquid nitrogen. Cryosections were made at  $-110^\circ\text{C}$  using a diamond knife (Diatome, Bienne, Switzerland) and immunolabeling on the cryosections was performed as described previously (Griffiths et al., 1984). Gold-labeled goat anti-IgGs were used as secondary antibodies (Janssen, Olen, Bel-

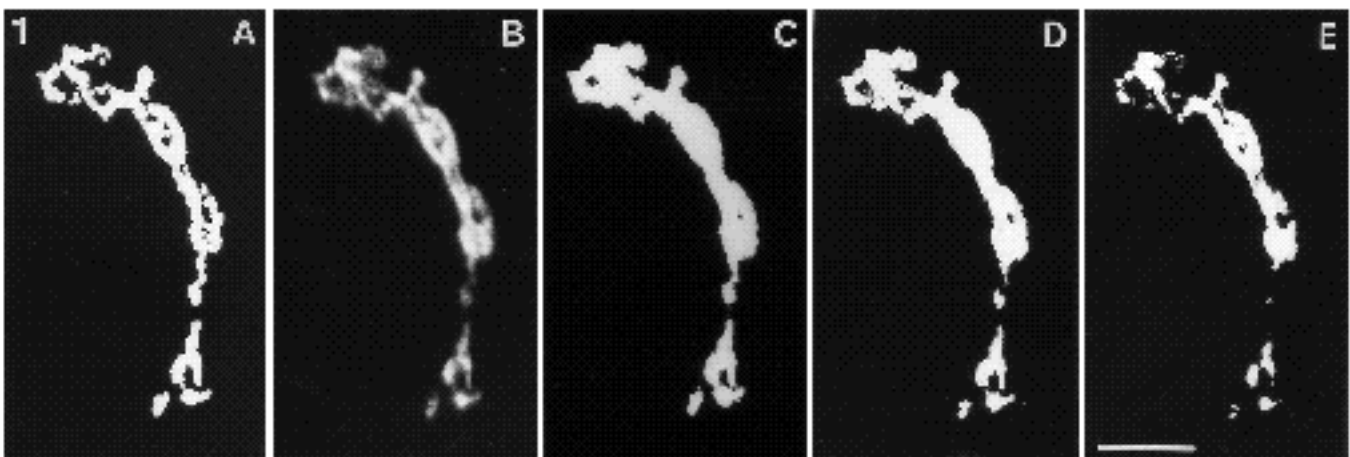


**Fig. 1.** Comparison between the top hat filter and a simple threshold filter. The mask obtained using the top hat filter (A) can be compared with the original image (B) and with a set of masks obtained by using simple threshold filters (C-E). (C) Threshold filter (30-255); (D) threshold filter (45-255); (E) threshold filter (60-255). The mask obtained using the top hat filter fits better the detailed pattern of the original image than those obtained with the simple threshold filter. Bar,  $5 \mu\text{m}$ .

gium). Finally, the cryosections were observed in a Philips EM410 at 80 kV.

## Results

### *Compartments of the Golgi apparatus can be visualized at the CLSM level*

In the first step, it was necessary to find out whether our approach, using a confocal microscope, could provide reliable morphological information on the relative positions of already characterized markers within the Golgi apparatus. The Golgi apparatus is composed of a set of morphologically and functionally discrete compartments and the size of these elementary units is close to the limit of the spatial resolution of the optical microscope ( $= 0.2 \mu\text{m}$ ). Theoretically, two consecutive cisternae can be distinguished by use of the appropriate biochemical markers. Therefore, double-labeling experiments of chosen Golgi compartments with appropriate markers should permit the observation of two distinct or mixed staining patterns, according to the relative position of the selected markers, colocalized or not.

Since only a restricted number of antibodies raised against Golgi antigens are available (and many of them are species-specific), we had little choice in selecting the most convenient markers for double-labeling experiments. Morphologically, the absolute specificity of a marker is dependent upon the accuracy with which this antigen has been localized. In this respect, the best-defined antibody we used was the rabbit antiserum raised against TGN38, an integral membrane protein associated with the TGN (Luzio et al., 1990). Recent data indicate that TGN38 might in fact shuttle between TGN and endosomal compartments (Reaves and Banting, 1992; Lippincott-Schwarz et al., 1991); nevertheless at steady state TGN38 appears to be restricted to the TGN. Concerning the opposite side of the Golgi, we chose to use a polyclonal antibody that recognizes an integral membrane protein bound to *cis* and medial Golgi apparatus (GIMP<sub>c</sub>) (Yuan et al., 1987). If this antigen is distributed over more than the sole *cis* compartment, this antibody is nevertheless a valuable marker of the *cis* side of the Golgi apparatus. Finally, we chose a third antibody, the monoclonal 53FC3, that recognizes a 135 kDa antigen (Burke et al., 1982), mannosidase II (Baron and Garoff, 1990). This enzyme is thought to be located in medial cisternae, according to biochemical data; however, the morphological data indicate that it localizes in very few central cisternae (Burke et al., 1982). Still, it is often considered as a suitable marker for medial cisternae of the Golgi apparatus.

Double-labeling experiments were performed on NIH 3T3 cells because it was the only cell line tested in which all these markers could be detected. Two pairs of markers, considered as topological references, were first compared: mannosidase II (medial) with GIMP<sub>c</sub> (*cis*-medial) or TGN38 (TGN). These couples of antigens were chosen because they should colocalize in the first case while they should be separate in the second (Fig. 2A, B) if the distribution of each antigen is uniform and restricted to given Golgi compartments.

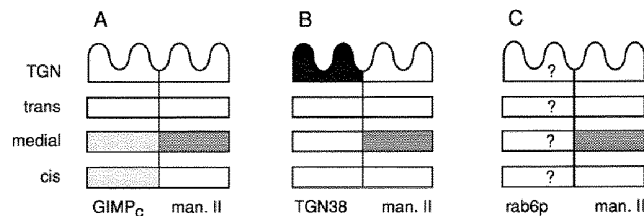
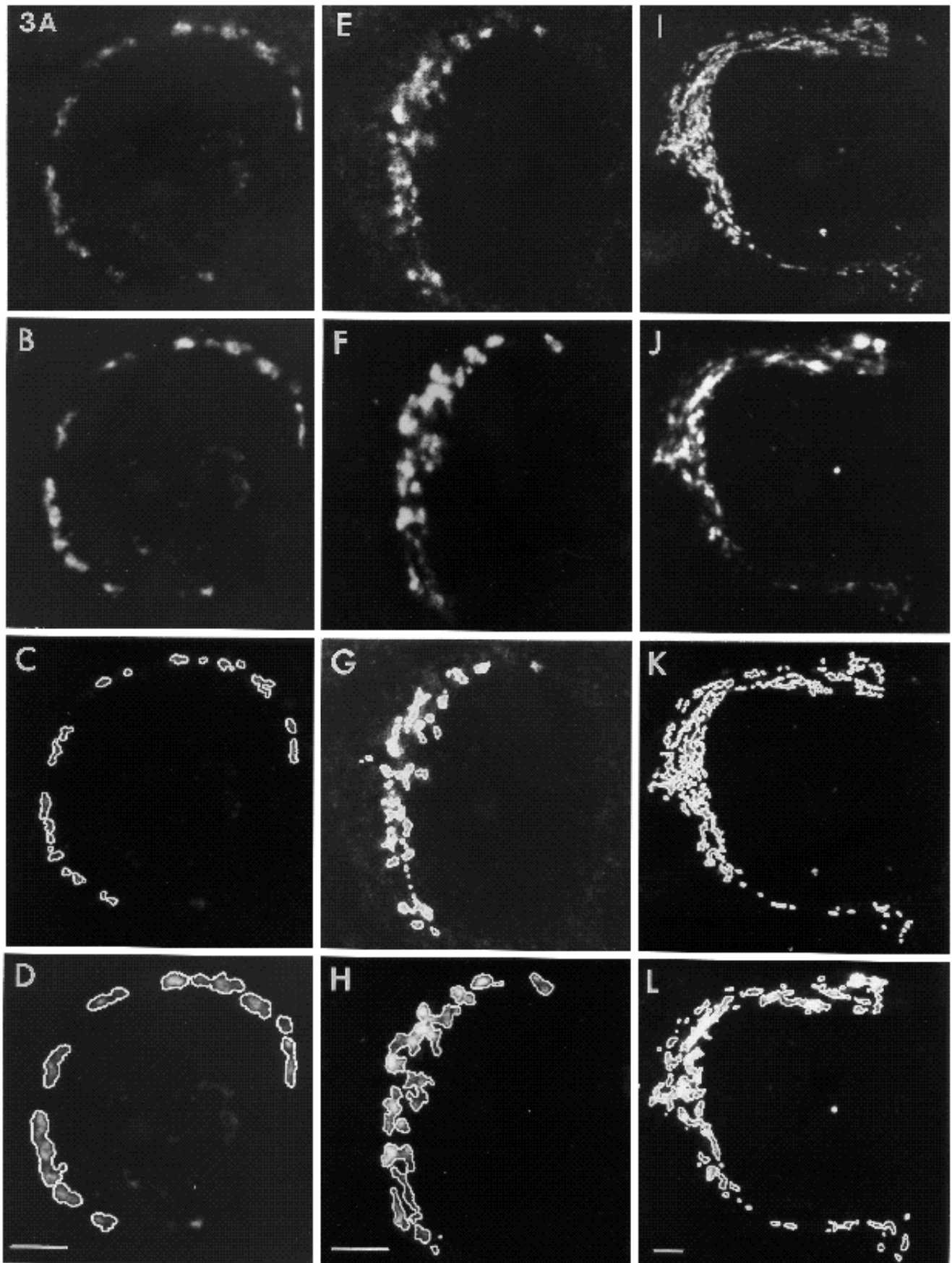


**Fig. 2.** Schematic representation of the relative position of Golgi marker couples used as a reference to identify rab6p localization. (A) Theoretical colocalization configuration with mannosidase II and GIMP<sub>c</sub>. (B) Theoretical separation configuration with mannosidase II and TGN38. (C) Experimental situation with mannosidase II and rab6p, the distribution of which is to be determined.

When the distribution of these reference markers was investigated by CLSM under optimum conditions (see Materials and methods), slight differences in the staining patterns were noticed in the first pair (mannosidase II/GIMP<sub>c</sub>; Fig. 3A, B) while clear differences were observed in the second (mannosidase II/TGN38; Fig. 3E, F). To analyze further the extent of colocalization, the images from both channels were merged (Fig. 4A-D). The relative distribution of the two antigens is defined according to a palette using three colors: red, green and yellow. Red and green correspond not only to single-stained areas, but also to overlapping areas with unbalanced gray levels. Yellow pixels (red and green mixed at a single pixel level) can be observed only if the ratio between the gray levels of the corresponding pixels in the two images is close to unity, and if the red and green values are within the 100-255 range (see the test card coupled to the images). The factor limiting the interpretation of the color palette in the merged images is the dynamic range of the original images, which is defined during image acquisition and depends upon the following parameters: the local concentration of the fluorophores in the specimen, the adjustment of the microscope (photomultiplier, laser, etc.), the filters used to select the light emitted by the fluorophores, the quantic efficiency, etc... Moreover, the adjustment of both the chrominance and the luminance of the merged images is very difficult, because adjustments in one of the channels (red or green) change the balance between the colors and modify the values of the yellow pixels (i.e. the overlapped areas).

Therefore, to analyze and compare the staining patterns, we defined the areas of interest by segmentation (see Materials and methods). The outlined pictures show the contours

**Fig. 3.** Relative distribution of the mannosidase II medial marker in the Golgi apparatus compared with either reference markers with opposite polarities (TGN 38 or GIMP<sub>c</sub>) or rab6p as observed by confocal microscopy on double-stained 3T3 cells (as described in Materials and methods). Optical sections showing the original patterns of staining obtained for mannosidase II (A, red channel) and GIMP<sub>c</sub> (B, green channel); mannosidase II and TGN 38 (E, F), and mannosidase II and rab6p (I, J). The outlines that delimit the biologically significant areas were obtained by a thresholding step (top hat filter, see Materials and methods) and superimposed on the corresponding original images as a validation test: mannosidase II and GIMP<sub>c</sub> (C, D); mannosidase II and TGN 38 (G, H) and mannosidase II and rab6p (K, L). Bars, 5  $\mu\text{m}$ .



of the areas considered to be biologically significant (Fig. 3C, D, G, H). Merges of the resulting binary images can be compared with those of the original pictures and allowed a better interpretation of the overlap (Fig. 4A-D). The merge of the binary images for the pair GIMP<sub>c</sub>/mannosidase II revealed an obvious colocalization of these two markers, since the mannosidase II staining pattern appeared to be totally included in the GIMP<sub>c</sub> staining pattern (Fig. 4B). On the other hand, the GIMP<sub>c</sub> staining pattern appears to spread around the overlap (Fig. 4B). This was confirmed when the areas of overlap were quantified (see Materials and methods). The quantification showed that almost 100% of the mannosidase II staining (red) was included in the GIMP<sub>c</sub> staining (green, Fig. 5A) while 62% of the compartment defined by the GIMP<sub>c</sub> labeling was single stained. These data all indicate unambiguously, and better than the merge of the original images does, that the mannosidase II staining pattern is included within the GIMP<sub>c</sub> staining pattern, in good agreement with the expected localization of these markers (Baron and Garoff, 1990; Burke et al., 1982; Yuan et al., 1987).

When the second pair of reference markers (mannosidase II and TGN38; Fig. 2B) was subjected to the same analysis, differences were observed between the two staining patterns (Fig. 3E-H). The merge of the binary images showed clear dissimilarities between the two staining patterns (Fig. 4D). However, an area of overlap was observed but only concerned a small part of the overall image as shown by the quantification of this area (Fig. 5B): 77% of the area corresponding to TGN38 and 35% of the area corresponding to mannosidase II were excluded from the overlap.

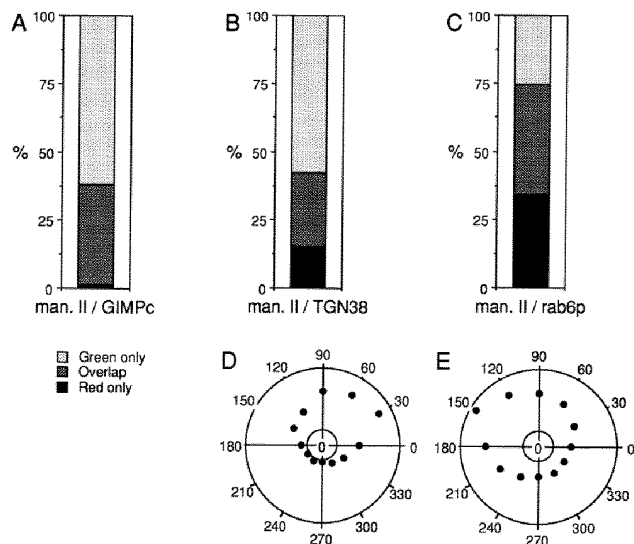


**Fig. 5.** Quantification of the single-stained areas and of the overlap in the binary merges. (A) Mannosidase II/GIMP<sub>c</sub>; (B) mannosidase II/TGN38; and (C) mannosidase II/rab6p. The orientation of the TGN38 pattern of staining with regard to the overlap using the compass-card method (D) establishes and records the polarity of the Golgi apparatus (see Materials and methods). The application of this method to the orientation of rab6p staining with regard to the overlap shows a polarized distribution of rab6p on the TGN side of the Golgi apparatus (E).

Thus, the comparison of the distribution of characterized Golgi markers in our experimental conditions showed that the CLSM analysis permits us to distinguish between various Golgi compartments.

#### *rab6p is localized on the trans side of the Golgi apparatus*

The CLSM approach was then used to localize rab6p, using the medial Golgi marker (mannosidase II) as a reference (Fig. 2C). Like the mannosidase II/TGN38 couple, the original images display dissimilarities between rab6p and mannosidase II staining patterns (Fig. 3I-L). The observation of the binary images led to the same conclusion (Fig. 4E-F). The quantification of the overlap area and the single-stained areas (Fig. 5C) gave results similar to those obtained for the mannosidase II/TGN38 couple (Fig. 5B), since about 50% of the rab6p or mannosidase II staining pattern was excluded from the overlap.

However, the orientation of the rab6p/mannosidase II pair remains to be determined with regard to the polarity of the Golgi apparatus. The compass-card analysis (see Materials and methods) applied to both pairs enabled us to determine whether rab6p is located on the same side of the Golgi apparatus as TGN38 or on the opposite side. The compared compass-card diagrams, shown in Fig. 5 (D-E), indicate that rab6p is distributed on the same side of the overlap as TGN38.

The data for the distribution of rab6p and its polarized orientation with regard to mannosidase II strongly suggest that rab6p partially colocalizes with mannosidase II and is also located on the TGN side of the Golgi apparatus.

#### *Statistical analysis*

All the previous results were shown on single images. To assess the validity of our approach, we performed a statistical analysis on series of images (6-10, see Fig. 6) corresponding to the three pairs of markers described above. When we analyzed the respective size of the single-stained areas and of the overlap in the binary merges from indi-

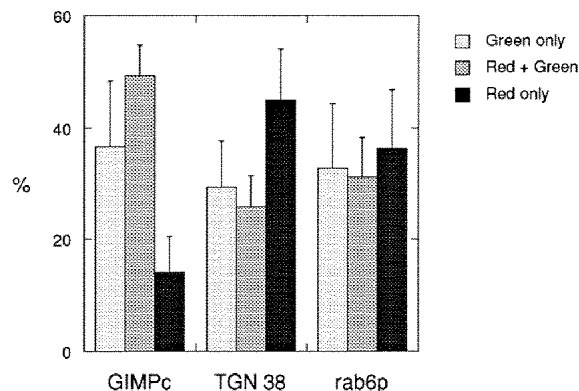


**Fig. 6.** Statistical analysis of the quantification of the single-stained areas and of the overlap in the binary merges from individual sections obtained on different Golgi apparatus. The marker's couples are mannosidase II/GIMP<sub>c</sub> (GIMP<sub>c</sub>); mannosidase II/TGN38 (TGN38); and mannosidase II/rab6p (rab6p). The number of images used was 6 for GIMP<sub>c</sub>, 7 for TGN38 and 10 for rab6p. Red, mannosidase II; green, GIMP<sub>c</sub>, TGN38 or rab6p. Error bars correspond to the standard deviation.

vidual sections obtained on different Golgi apparatus, we found results similar to those obtained on single sections (Fig. 6). The statistical analysis of the compass card from individual sections obtained on different Golgi apparatus showed that TGN 38 and rab6p were located on the same side of the Golgi apparatus (Fig. 7).

#### *rab6p colocalizes with the VSV-G protein within the TGN*

As rab6p seems to be at least partially localized on the *trans* side of the Golgi apparatus, its actual distribution relative to the *trans*-most side of the organelle requires further investigation. For technical reasons, direct comparison of the localization of rab6p and TGN38 was not possible, since both antibodies were raised in rabbits. Therefore, we chose to use the VSV (vesicular stomatitis virus)-infected cell system (Matlin and Simons, 1983). The VSV-G protein from the tsO45 mutant strain of VSV can be used as a dynamic marker of the exocytic pathway, since this protein is bound to ER membranes in cells kept at 39.5°C, while it specifically accumulates in the TGN when the temperature is shifted to 20°C (Griffiths et al., 1985; Matlin and Simons, 1983). Thus, we used VSV-infected BHK cells to compare the localization of rab6p and VSV-G in cells cultured at both temperatures.

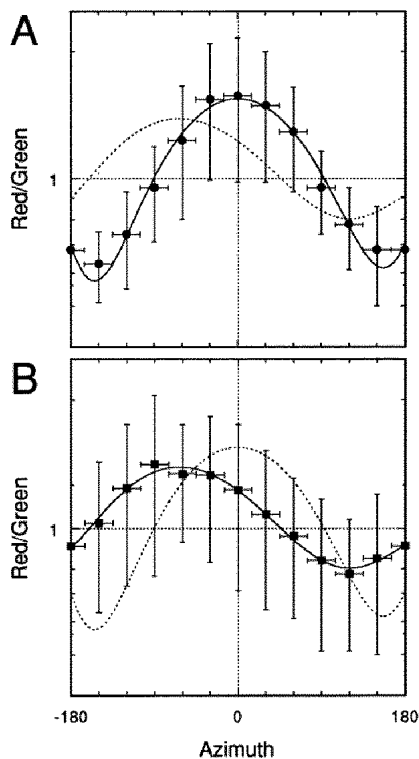


**Fig. 7.** Statistical analysis of the compass card from individual sections obtained on different Golgi apparatuses. The marker's couples are mannosidase II/TGN38 (top) and mannosidase II/rab6p (bottom). The number of images used was 7 for mannosidase II/TGN38 and 10 for mannosidase II/rab6p. Error bars correspond to the standard deviation in the x axis and to the uncertainty in the y axis ( $\pm 15^\circ$ ) due to the determination of the orientation of the Golgi apparatus (on an hexagonal grid). The curves were fitted using a polynomial curve fit (polynomial order = 5) with  $r = 0.99$ .

At 39.5°C, the distribution of the VSV-G protein in the cytoplasm was extensive as seen with a conventional epifluorescence microscope (Fig. 8A). In contrast, rab6p showed clearly a typical Golgi staining pattern, quite distinct from the ER staining pattern observed with VSV-G (Fig. 8B). However, at 20°C, the patterns observed with both proteins were very similar and they looked like a Golgi pattern (Fig. 8C, D).

To analyze more precisely the relative distribution of these two proteins at both temperatures, a CLSM analysis was performed at selected levels within the cells, where both stainings were present. The images were segmented and the binary images were merged (see Materials and methods). At 39.5°C, rab6p (Fig. 9A, white, 56%) was clearly separated from VSV-G (Fig. 9A, dark gray, 78%) with only a small area of overlap (Fig. 9A, light gray). At 20°C, a striking colocalization of rab6p and VSV-G was observed (Fig. 9B). Quantification of the VSV-G (dark gray), rab6p (white) and overlap areas (light gray) was performed (Fig. 10): at 39.5°C the greater part of the rab6p (56%) and VSV-G (78%) areas did not overlap, while at 20°C almost all the rab6p staining (94%) is included within the TGN compartment as defined by the VSV-G staining.

This experiment strengthens our previous observation suggesting that rab6p is associated with the TGN at the exit of the Golgi apparatus.

#### *Electron microscopy supports the CLSM data*

Although the observations reported above were made at the optical microscope resolution (CLSM), we obtained detailed information about the organization of the Golgi apparatus, which is more usually provided by EM investigations. To reinforce the validity of our observations, we have investigated the localization of rab6p in NIH 3T3 cells and in VSV-infected BHK cells by EM using labeled cryosections.

In NIH/3T3 cells, rab6p is found associated with the Golgi apparatus. Obviously, some cisternae of the Golgi stacks were labeled, but gold particles were also found near the stacks (Fig. 11A). Thus, simple labeling using rab6p antibodies indicates that this protein spreads over more than just a few restricted cisternae. Therefore, it was necessary to check also by EM the colocalization of rab6p with VSV-G in BHK cells blocked at 20°C. During the 20°C block, the VSV-G protein accumulates in a tubulovesicular network characteristic of the TGN (Fig. 11B, C). rab6p and VSV-G were found within the same membranes, although the rab6p labeling was less abundant. As indicated by the gold particle labeling, rab6p is also associated with flat cisternae in the Golgi stacks, where some VSV-G proteins are detectable as well.

Thus, rab6p appears to spread over several discrete compartments as far as these can be distinguished using VSV-G as a TGN marker. These EM observations support and therefore validate the CLSM data on rab6p localization in the Golgi apparatus.

## Discussion

rab6p is a small GTP-binding protein belonging to the exo-



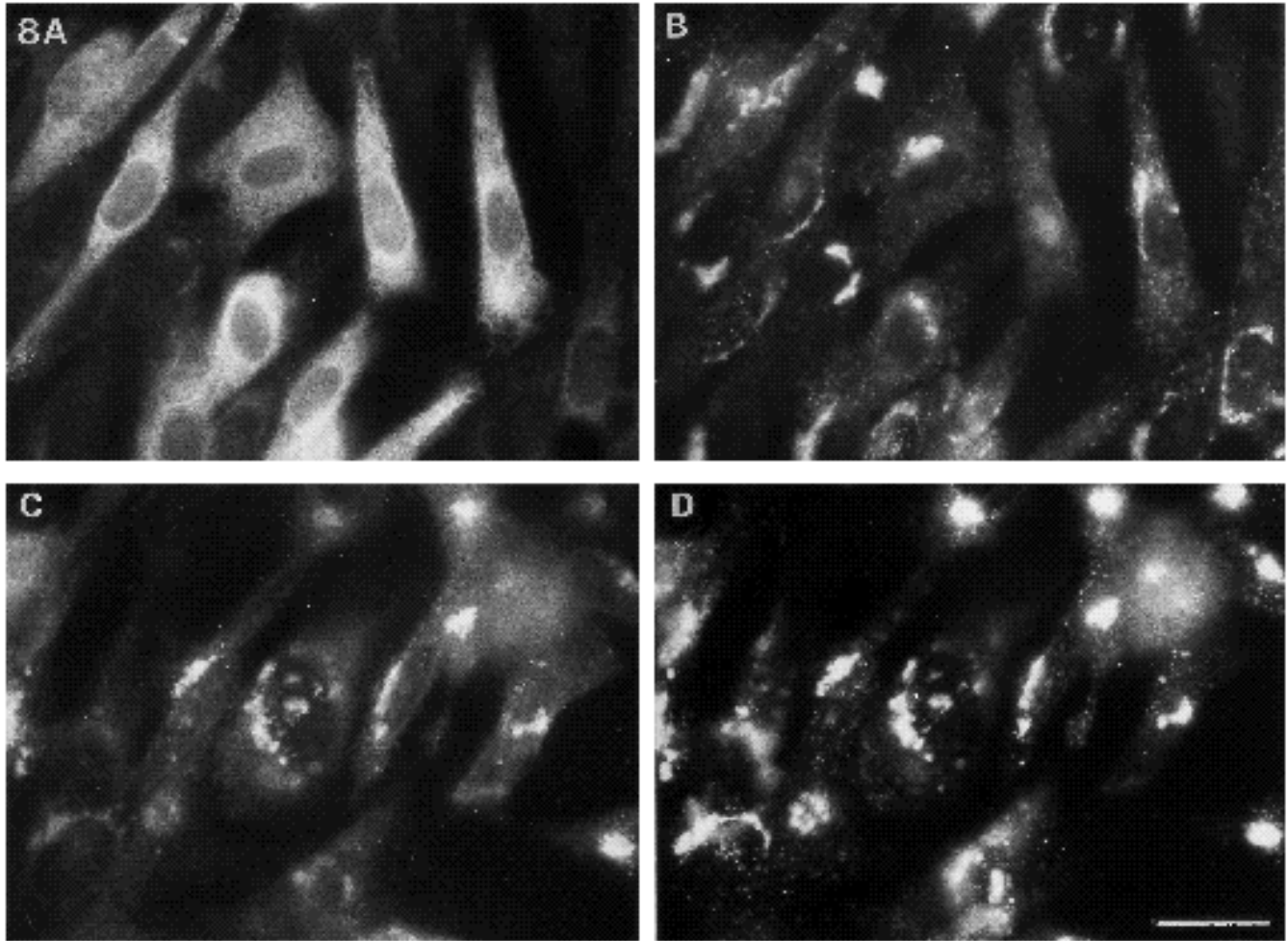


**Fig. 8.** Compared localization of rab6p and VSV-G in infected BHK cells, by conventional immunofluorescence. At 39.5°C VSV-G is localized in the ER (A) while rab6p staining is clearly concentrated in the Golgi area (B). After shifting the temperature to 20°C, VSV-G moves to the TGN where it specifically accumulates (C). The staining patterns of both antigens then look very similar. Therefore rab6p seems to colocalize with VSV-G during this 20°C block (D). Bar, 10 µm.

cytic pathway. Its association with the Golgi apparatus has been previously established (Goud et al., 1990). In this study we focused on the detailed determination of rab6p localization within the Golgi apparatus to try and understand this protein's site of function more precisely. We have shown that one can distinguish, by CLSM, between various compartments of the Golgi apparatus defined by specific markers. Using this approach we were able to show that rab6p is present in the TGN as well as in the flat cisternae of the Golgi apparatus.

#### *Distinction between Golgi markers by CLSM*

Optical sections performed in double-labeled cells with known markers of the Golgi apparatus provided the basic information which we attempted to interpret in terms of morphology. Three types of situations were expected regarding the relative distribution of the pairs of markers: a full coincidence (colocalization), a full separation (no colocalization), or a partial colocalization (overlap). Although the first two situations can be easily interpreted,

the latter raises the problem of the origin of the overlap.

Owing to the size of the Golgi compartments, which is very close to the resolution of the CLSM, we had to define acquisition conditions to oversample in the (*x*, *y*) plane and in the *z* direction. However, even under such conditions, an overlap between the two staining patterns was always observed in the merge of the original images. This overlap proved to be difficult to analyze precisely, for several reasons. Indeed, in the merges of the original fluorescein and rhodamine images, the ratio between the green and the red levels in the coincident pixels was variable and could lead to confusing interpretations. Among the pixels belonging to the overlap, some could be interpreted as clearly corresponding to the overlap (colored in yellow), while others could not be identified when one color is outweighed by the other, thus leading to an underestimation of their number. Moreover, the fluorescence intensity in the green or red channel depended not only on the local concentration of the particular antigens but also on many other factors (see Results).



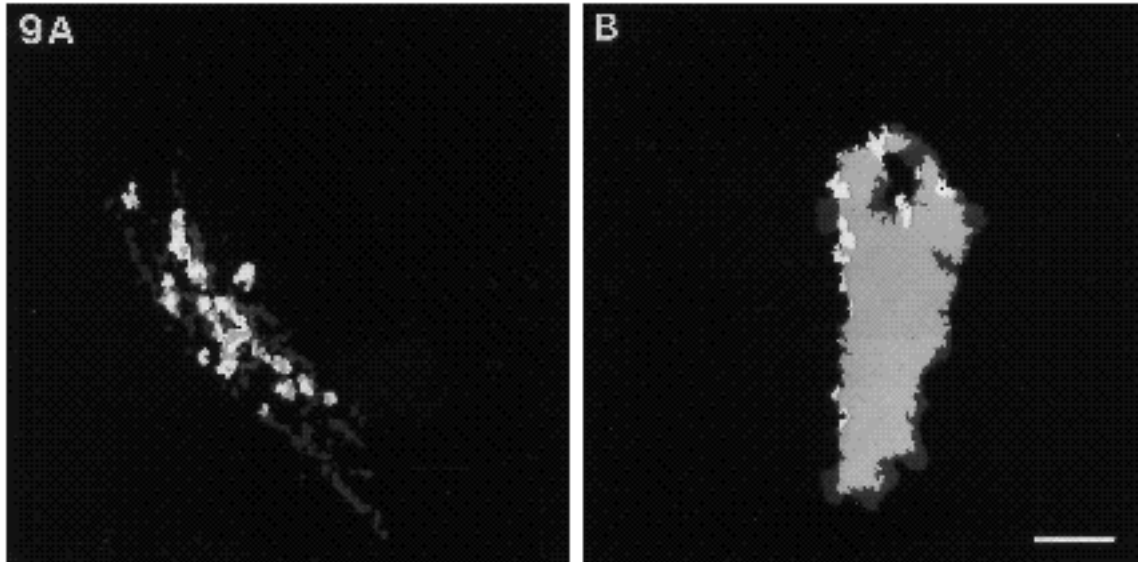


**Fig. 9.** LSCM pictures of VSV-infected BHK cells double-labeled for VSV-G and rab6p. An optical section through a cell grown at 39.5°C (when VSV-G is blocked in the ER) in which both labelings were present was selected: different staining patterns were observed for VSV-G and rab6p (A). At 20°C a section across the Golgi complex shows the colocalization of rab6p with VSV-G filling the TGN (B). White, rab6p; dark gray, VSV-G; light gray, overlap. Bar, 5  $\mu$ m.

For these reasons and to obtain the most precise possible interpretation of the overlap between the two original pictures, we chose to merge the binary images corresponding to the biologically significant areas (i.e. the areas of interest defined in the original images, independently for the two channels, and systematically validated by superimposition of the binary outlines on the original images). Various threshold levels ("top hat" filter) were tested to define the binary images. No significant variations in the data described hereafter were recorded. Moreover, this analysis provides quantitative information that helps in the interpretation of the merges of the original images. Finally, when a statistical analysis was performed on a series of images from different Golgi apparatuses, similar results were obtained.

Under these conditions we observed, as expected, the inclusion of the mannosidase II staining pattern within that of the GIMP<sub>c</sub>, whereas part of the GIMP<sub>c</sub> pattern was found to be excluded from the mannosidase II-stained area. The quantification data totally supported these results. In contrast, mannosidase II and TGN38 showed only a restricted overlapping area, the quantification of which clearly demonstrated that we can distinguish experimentally between two theoretically distinct situations. We think that it is the combination of both the limitations of the CLSM and the scale of organization of the Golgi cisternae that led to the usual observation of a small overlap, thus causing possible confusion between two closely related but distinct antigens. However, we cannot exclude a partial colocalization of the compared antigens.

#### *Distribution of rab6p in Golgi compartments and in the TGN*

The CLSM data comparing the rab6p/mannosidase II and

TGN38/mannosidase II pairs indicate that rab6p has a polarized distribution, on the same side of the Golgi complex as TGN38. These results confirmed the previous finding of a polarized distribution of rab6p in NRK cells (Goud et al., 1990). As a direct comparison of rab6p and TGN38 localization was not possible in the same cell (due to the nature of the antibodies), we checked the localization of rab6p in VSV-infected BHK cells blocked at 20°C. CLSM analysis showed unambiguously that rab6p and VSV-G colocalized at 20°C (in the TGN), in contrast with what was observed at 39.5°C. The EM data further confirmed the precise colocalization of rab6p with the VSV-G protein in the TGN and showed as well that rab6p is not present solely in this compartment but is also present in cisternae next to the TGN.

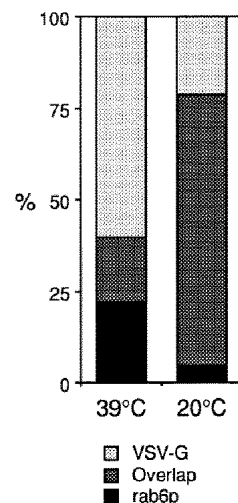


**Fig. 10.** Quantification of the overlaps between VSV-G and rab6p patterns of staining at 39.5°C when VSV-G is blocked in the ER and during the 20°C block. The data correspond to the area measurements of the images in Fig. 8.

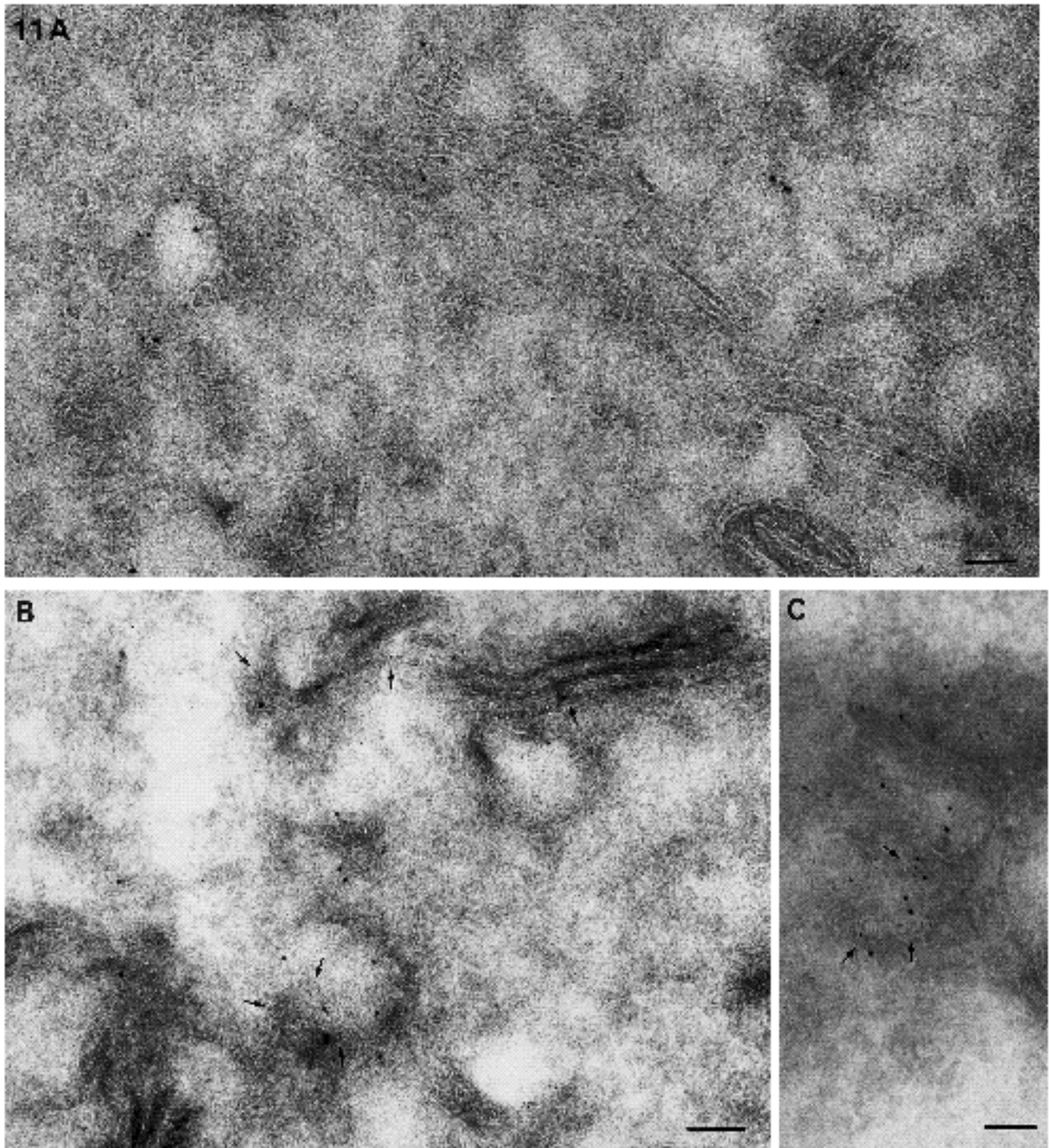


**Fig. 11.** EM localization of rab6p by immunogold labeling on cryosections. (A) Frozen thin section of NIH/3T3 cells showing rab6p labeling associated with Golgi membranes. The gold particles (10 nm) are found on the membrane of the Golgi cisternae as well as on membranes forming a network related to the Golgi stack. (B,C) BHK cells were infected with VSV tsO45, maintained at 39.5°C for 3 h, and shifted to 20°C for 2 h. rab6p labeling (5 nm gold particles) colocalizes with VSV-G protein (10 nm gold particles) in areas on the rim of the Golgi stack (arrows) where TGN-tubulovesicular structures are identified by the VSV-G labeling (C). Bars, 100 nm.

In a previous study, a polarized localization of rab6p was shown within the Golgi complex in NRK cells (Goud et al., 1990). These results were based on reference markers of the *cis* side and medial aspect of the Golgi complex and

no further investigations using *trans* or TGN markers were performed. The present study shows that the distribution of rab6p extends over at least the medial and *trans*-Golgi cisternae and the TGN in NIH/3T3 and BHK cells. rab6p is

a ubiquitous protein and it is likely that it displays the same localization in different cell types. However, more detailed investigations will be necessary to confirm this.

Since the TGN is the site of assembly of transport vesicles destined for the plasma membrane or other intracellular organelles, one can ask whether rab6p is also associated with post-Golgi transport vesicles. In BHK cells, but also in other cell types, a punctate staining is observed with anti-rab6p antibodies (refer to Fig. 5B), which may reflect the staining of post-Golgi vesicles, although their characterization may prove to be difficult. Nevertheless, in cell types where post-Golgi vesicles can be identified, such as neurons (Tixier-Vidal et al., unpublished data) or electrocytes of *Torpedo marmorata* (Jasmin et al., 1992), rab6p has been shown to associate with these vesicles.

#### *Biological significance of rab6p localization*

The localization of Sec4/Ypt1/rab proteins associated with distinct exocytic or endocytic compartments has been interpreted so far to support the hypothesis that these proteins play a role in specific targeting/fusion events. According to Bourne's model, the function of these proteins would be to monitor the targeting/fusion events to the correct acceptor compartment (Bourne, 1988). However, functional data do not completely support this hypothesis. Indeed, Ypt1p seems to function in both ER-to-Golgi and intra-Golgi transport events (Bacon et al., 1989; Baker et al., 1990; Segev, 1991). Similarly, rab1bp, one of the mammalian homologues of Ypt1p, is also involved in several transport steps between ER and Golgi subcompartments (Plutner et al., 1991). Although the function of rab6p is unknown, the localization data now available for rab6p favor the hypothesis that rab6p functions in intra-Golgi as well as early post-Golgi transport events. These data all suggest that at least some of the Sec4/Ypt1/rab proteins regulate a series of events occurring at various stages of intracellular transport, rather than a specific targeting/fusion event.

We thank Drs. P. Luzio (MRC Cambridge, UK), B. Burke (Harvard Medical School, Boston, USA), I. Sandoval (Centro de Biología Molecular, Madrid, Spain) for the generous gift of antibodies against intrinsic Golgi membrane proteins, Drs. T. Kreis and G. Griffiths for the gift of P5D4 antibody and Dr. F. Laffay (CNRS, Gif-sur-Yvette) for the gift of tsO45 strain. We are grateful to R. Schwarztman for expert photographic assistance. This work was supported by grants from Fondation pour la Recherche Médicale, Ligue Nationale contre le Cancer, Association pour la Recherche contre le Cancer and Institut National pour la Santé et la Recherche Médicale to B.M. and grants from Fondation pour la Recherche Médicale, Ligue Nationale contre le Cancer and Université Pierre et Marie Curie to B.G.

#### References

Bacon, R. A., Salminen, A., Ruohola, H., Novick, P. and Ferro-Novick, S. (1989). The GTP-binding protein YPT1 is required for transport in vitro: the Golgi apparatus is defective in YPT1 mutants. *J. Cell Biol.* **109**, 1015-1022.

Baker, D., Wuestehube, L., Schekman, R., Botstein, D. and Segev, N. (1990). GTP-binding Ypt1 protein and Ca<sup>2+</sup> function independently in a cell-free protein transport reaction. *Proc. Nat. Acad. Sci. USA* **87**, 355-359.

Baron, M. D. and Garoff, H. (1990). Mannosidase II and the 135K-Da

Golgi-specific antigen recognized by monoclonal antibody 53FC3 are the same dimeric protein. *J. Biol. Chem.* **265**, 19928-19931.

Bourne, H. R. (1988). Do GTPases direct membrane traffic in secretion? *Cell* **53**, 669-671.

Burke, B., Griffiths, G., Reggio, H., Louvard, D. and Warren, G. (1982). A monoclonal antibody against a 135-k Golgi membrane protein. *EMBO J.* **1**, 1621-1628.

Chavrier, P., Parton, R. G., Hauri, H. P., Simons, K. and Zerial, M. (1990a). Localization of low-molecular weight GTP-binding proteins to exocytic and endocytic compartments. *Cell* **62**, 317-329.

Chavrier, P., Vingron, M., Sander, C., Simons, K. and Zerial, M. (1990b). Molecular cloning of YPT1/SEC4-related cDNAs from an epithelial cell line. *Mol. Cell. Biol.* **10**, 6578-6585.

Fischer von Mollard, G., Südhof, T. C. and Jahn, R. (1991). A small GTP-binding protein dissociates from synaptic vesicles during exocytosis. *Nature* **349**, 79-82.

Gallwitz, D., Donath, C. and Sander, C. (1983). A yeast gene encoding a protein homologous to the human c-ras/bas proto-oncogene. *Nature* **306**, 704-707.

Gorvel, J.-P., Chavrier, P., Zerial, M. and Gruenberg, J. (1991). rab5 controls early endosome fusion in vitro. *Cell* **64**, 915-925.

Goud, B. and McCaffrey, M. (1991). Small GTP-binding proteins and their role in transport. *Curr. Opin. Cell Biol.* 626-633.

Goud, B., Salminen, A., Walworth, N. and Novick, P. (1988). A GTP-binding protein required for secretion rapidly associates with secretory vesicles and the plasma membrane in yeast. *Cell* **53**, 753-768.

Goud, B., Zahraoui, A., Tavittian, A. and Saraste, J. (1990). Small GTP-binding protein associated with Golgi cisternae. *Nature* **345**, 553-556.

Griffiths, G., McDowall, A., Back, R. and Dubochet, J. (1984). On the preparation of cryosections for immunocytochemistry. *J. Ultrastruct. Res.* **65**, 78-89.

Griffiths, G., Pfeiffer, S., Simons, K. and Matlin, K. (1985). Exit of newly synthesized membrane proteins from the trans cisternae of the Golgi complex to the plasma membrane. *J. Cell. Biol.* **101**, 949-964.

Haubruck, H., Prange, R., Vorgias, C. and Gallwitz, D. (1989). The ras-related mouse ypt1 protein can functionally replace the YPT1 gene product in yeast. *EMBO J.* **8**, 1427-1432.

Inoue, S. (1986). *Video Microscopy*, section 10.4, pp. 334-338. New York, London: Plenum Press.

Jasmin, B. J., Goud, B., Camus, G. and Cartaud, J. (1992). The low molecular weight GTP-binding protein rab6p associates with distinct post-Golgi vesicles in *Torpedo marmorata* electrocytes. *Neuroscience* **4**, 849-855.

Kreis, T. E. (1986). Microinjected antibodies against the cytoplasmic domain of vesicular stomatitis virus glycoprotein block its transport to the cell surface. *EMBO J.* **5**, 931-941.

Lippincott-Schwarz, J., Yuan, L., Tipper, C. Amherdt, M., Orci, L., and Klausner, R. D. (1991). Brefeldin A's effects on endosomes, lysosomes and the TGN suggests a general mechanism for regulating organelle structure and membrane traffic. *Cell* **67**, 601-616.

Luzio, J. P., Brake, B., Banting, G., Howell, K. E., Braghetta, P. and Stanley, K. K. (1990). Identification, sequencing and expression of an integral membrane protein of the trans-Golgi network (TGN 38). *Biochem. J.* **270**, 97-102.

Matlin, K. S. and Simons, K. (1983). Reduced temperature prevents transfer of membrane glycoproteins to the cell surface but does not prevent terminal glycosylation. *Cell* **34**, 233-243.

Palade, G. (1975). Intracellular aspects of the process of protein synthesis. *Science* **189**, 347-358.

Pfeiffer, S. R. (1992). GTP-binding proteins in intracellular transport. *Trends Cell Biol.* **2**, 41-45.

Plutner, H., Cox, A., Pind, S., Khosravi-Far, R., Bourne, J., Schwaninger, R., Der, C. and Balch, W. (1991). Rab1b regulates vesicular transport between the endoplasmic reticulum and successive Golgi compartments. *J. Cell Biol.* **115**, 31-43.

Reaves, B. and Banting, G. (1992). Perturbation of the Morphology of the trans-Golgi Network following Brefeldin A Treatment: Redistribution of a TGN-specific Integral Membrane Protein, TGN38. *J. Cell Biol.* **116**, 85-94.

Rothman, J. E. and Orci, L. (1992). Molecular dissection of the secretory pathway. *Nature* **355**, 409-415.

Salminen, A. and Novick, P. (1987). A ras-like protein is required for a post-Golgi event in yeast secretion. *Cell* **47**, 527-538.

Segev, N. (1991). Mediation of the attachment or fusion step in

- vesicular transport by the GTP-binding Ypt1 protein. *Science* **252**, 1553-1556.
- Segev, N., Mulholland, J. and Botstein, D.** (1988). The yeast GTP-binding YPT1 protein and a mammalian counterpart are associated with the secretion machinery. *Cell* **52**, 915-924.
- Touchot, N., Chardin, P. and Tavitian, A.** (1987). Four additional members of the ras gene superfamily isolated by an oligonucleotide strategy: molecular cloning of YPT-related cDNAs from a rat brain library. *Proc. Nat. Acad. Sci. USA* **84**, 8210-8214.
- Walworth, N. C., Goud, B., Kabcenell, A. and Novick, P.** (1989). Mutational analysis of SEC4 suggests a cyclical mechanism for the regulation of vesicular traffic. *EMBO J.* **8**, 1685-1693.
- Webb, R. H. and Dorey, C. K.** (1990). The pixelated image. In *Handbook of Biological Confocal Microscopy* (ed. J. B. Pawley), pp. 41-51. New York: Plenum Publishing Corporation.
- Yuan, L., Barriocanal, J. G., Bonifacino, J. S. and Sandoval, I. V.** (1987). Two integral membrane proteins located in the cis-middle and transport of the Golgi system acquire sialylated N-linked carbohydrates and display different turnovers and sensitivity to cAMP-dependent phosphorylation. *J. Cell Biol.* **105**, 215-227.
- Zahraoui, A., Touchot, N., Chardin, P. and Tavitian, A.** (1989). The human Rab genes encode a family of GTP-binding proteins related to yeast YPT1 and Sec4 products involved in secretion. *J. Biol. Chem.* **264**, 12394-12401.

(Received 24 June 1992 - Accepted 27 July 1992)

9017 fig4 colour tip-in

**Fig. 4.** LSCM pictures comparing original and segmented merged images optical sections from doubly-stained 3T3 cells with known intrinsic Golgi markers and with rab6p. The rhodamine channel corresponds to mannosidase II, the green channel corresponds to GIMPc, TGN38 or rab6p staining. The merges of the original and binarized images are shown for mannosidase II/GIMPc (A,B), mannosidase II/TGN38 (C,D) and mannosidase II/rab6p (E,F), respectively. Bar, 5  $\mu$ m.